lytes. VI. Weak Electrolytes Including H_3PO_4," *J. Solution Chem.*, 5, 269 (1976).
Riesenfeld, F. C. and A. L. Kohl, *Gas Purification*, 2nd ed., Gulf Publishing Company (1974).
Silvester, L. F. and K. S. Pitzer, "Thermodynamics of Geothermal Brines, I. Thermodynamic Properties of Vapor-Saturated NaCl(aq) Solutions From 0-300°c," LBL-4456, University of California, Berkeley, California 94702 (1976).
Tosh, J. S., J. H. Field, H. E. Benson and W. P. Waynes, "Equilibrium Study of the System Potassium Carbonate, Potassium Bicarbonate, Carbon Dioxide and Water," U.S. Bureau of Mines, Report of Investigations, 5484 (1959).
Tsonopoulos, C., D. M. Coulson, and L. B. Inman, "Ionization Constants of Water Pollutants," *J. Chem. Eng. Data*, 21, 190 (1976).
Van Krevelen, D. W., P. J. Hoftijzer, and F. J. Huntjens, "Composition and Vapor Pressures of Aqueous Solutions of Ammonia, Carbon Dioxide, and Hydrogen Sulfide," Rec. Trav. Chim. Pays-bas, 68, 191 (1949).
Vega, R., and J. H. Vera, "Phase Equilibria of Concentrated Aqueous Solutions Containing Volatile Strong Electrolytes," *Can. J. Chem. Eng.*, 54, 245 (1976).
Walker, A. C., U. B. Bray and John Johnston, "Equilibrium in Solutions of Alkali Carbonates," *J. Am. Chem. Soc.*, 49, 1235 (1927).
Wen, C. Y., "Optimization of Coal Gasification Processes," Research and Development Report No. 66, Interim Report No. 1, Office of Coal Research, U.S. Dept. of the Interior (1971).

Manuscript received January 3, 1979; revision received May 14 and accepted June 5, 1979.

Calculation of Sulfate and Nitrate Levels in a Growing, Reacting Aerosol

THOMAS W. PETERSON

Department of Chemical Engineering
University of Arizona
Tucson, Arizona 85721

and

JOHN H. SEINFELD

Department of Chemical Engineering
California Institute of Technology
Pasadena, California 91125

The temporal variation of particle size and chemical composition of a marine aerosol exposed to SO_2, NH_3, NO, NO_2, H_2SO_4 and H_2O vapor is studied to determine the effect of these parameters on the sulfate and nitrate levels in the particle. Results show that, for gas phase SO_2 oxidation to sulfate, and liquid phase nitrate formation, those parameters that enhance sulfate formation tend to inhibit nitrate formation, and vice versa. Further, for the situation considered, the ratio predicted for sulfate and nitrate ions to ammonium ions is very nearly that found if all these ions were present in the form of NH_4NO_3 and $(NH_4)_2SO_4$. This compares favorably with data on sulfate, nitrate and ammonium levels in the Los Angeles area. The model used is capable of representing a general growing, reacting aerosol; other cases studied by this approach are briefly outlined. Limitations of its use are discussed.

SCOPE

The influence of atmospheric aerosols on human health and visibility depends on particle size and chemical composition. Three major particulate pollutants found in most urban regions are sulfates, nitrates and particulate hydrocarbons. These species are not, in general, emitted directly into the atmosphere, but rather are a consequence of chemical reactions involving emitted gaseous pollutants to form particulate species. These reactions take place by a number of mechanisms, such as homogeneous gas phase chemistry, heterogeneous solution chemistry, or surface catalyzed chemistry at the gas-particle interface. When condensation of water vapor accompanies these reactions, both the size and chemical composition of the aerosol may change.

Prediction of the size and chemical composition of a growing, reacting aerosol (given the primary particle size and composition and the concentration of various reactive gaseous pollutants) is central to the ability to mathematically model air pollutant behavior. Of particular importance is the ability to predict secondary sulfate and nitrate levels in the aerosol, since these are two of the major particulate components in both the urban and non-urban atmosphere. They appear in particles as a consequence of chemical reactions involving gaseous NO_x and SO_2. In this article, a model capable of predicting size and chemical composition of a growing, reacting aerosol particle is used to calculate the sulfate and nitrate levels of an initial marine aerosol, exposed to gaseous air pollutants.

CONCLUSIONS AND SIGNIFICANCE

Sulfate and nitrate levels in aqueous atmospheric aerosol particles, as well as particle size, are predicted as a function of exposure time for various ambient conditions. By considering a liquid phase nitrate formation mechanism and a gas phase sulfate formation mechanism, the following observations can be made:

1. Equilibrium conditions dictate that the ratio of nitrate and sulfate to ammonium ion, when all ions are present, is nearly that found in NH_4NO_3 and $(NH_4)_2SO_4$.

2. For the size range considered (0.05-2.0 μm radius), particle pH increases with particle size, the smallest particles being the most acidic. Particle pH ranges from approximately 1.75-3.0.

3. Those conditions which tend to increase sulfate concentration cause a decrease in nitrate concentration, and

Correspondence should be addressed to the first author.

vice versa. This implies that it could be possible to find sulfates and nitrates in different size fractions of the atmospheric aerosol, provided the mechanisms studied in this work are the important ones for ambient sulfate and nitrate formation.

The model derived can be used to study the chemistry and growth of atmospheric aerosols under other mechanisms and for other pollutant species, provided the necessary thermodynamic data for aqueous solutions are available.

Much work has been done to understand the complex chemistry that leads to secondary aerosol formation in the atmosphere. Of major interest is elucidating sulfate and nitrate formation mechanisms, since sulfates and nitrates not only often constitute a substantial fraction of the mass of atmospheric aerosols but also have been implicated in health-related aerosol effects. Reports of ambient sulfate and nitrate levels are numerous (Gordon and Bryan 1973, Charlson et al. 1974, Sandberg et al. 1976, Kadowaki 1976, Moskowitz 1977, Appel et al. 1978). Initial research aimed at explaining sulfate and nitrate relationships has been presented (Orel and Seinfeld 1977), although theoretical explanation of observed data with respect to relative levels of sulfates and nitrates and their dependences on particle size distribution is lacking.

The situation considered here is the formation of sulfates and nitrates in a "marine" aerosol particle. That is, we wish to study the growth rate and chemical speciation of an aerosol particle comprised initially of an equilibrium mixture of NaCl and $MgCl_2$ (the predominant salts in sea water) and exposed for a period of time to selected concentrations of gas phase pollutants. This model provides an idealized representation of processes that occur in the South Coast Air Basin of California, as moist salt-laden particles advect into the Basin. Gases to be considered are SO_2, NO, NO_2, NH_3 and H_2SO_4 vapor. By including H_2SO_4 vapor, we allow for the possibility of gas phase photochemical oxidation of SO_2.

A mathematical model developed to calculate simultaneous chemical reaction and particle growth of aerosols is described. We then apply the model to a specific mechanism of particle growth and chemical reaction for an initial "marine" aerosol. Prediction of relative compositions of sulfates, nitrates and ammonium is compared to those actually reported in the Los Angeles area.

GENERAL DESCRIPTION OF GROWING, REACTING AEROSOL

A complete description of the model utilized in this work can be found in Peterson and Seinfeld (1979). Basically, it allows for a full description of the processes by which vapor molecules transfer from the gas to the particulate phase. These processes include:

1) Transport from the bulk (gas) phase to the particle surface,

2) Transport across the gas-liquid interface,

3) Transport and chemical reaction within the liquid phase.

The next sections provide a brief summary of the mechanisms used to describe each of these three processes.

Transport from the Bulk Phase to the Particle Surface

Due to the wide range of particle diameters over which an atmospheric aerosol distribution varies (particle diameters between 0.001 and 10 μm), in the formulation of transport from the bulk phase to the surface, we must include a correction for noncontinuum transport based on the Knudsen number $Kn = \lambda/r$. A number of "transition regime" formulas have been proposed (Fuchs 1959, Brock 1966, Sampson and Springer 1969, Shankar 1970) to correctly describe transport to particles of all sizes; the interpolation formula derived by Sahni (1966) was chosen for this work. Particle growth by condensation of a single component can hence be described by (symbols are defined in the Nomenclature section).

$$\frac{dm}{dt} = \frac{1}{1 + lKn} \frac{4\pi r D}{RT_\infty} (p_\infty - p_c) \tag{1}$$

$$l = \frac{4/3 + 0.71\, Kn^{-1}}{1 + Kn^{-1}} \tag{2}$$

Transport Across the Gas-Liquid Interface

Two factors influence the equilibrium surface pressure above an aerosol droplet: the Kelvin effect and the solute effect. The Kelvin effect describes the relationship between the equilibrium vapor pressure of a component over a flat surface, and that over a curved surface. It is written as:

$$p_{ci} = p_{fi} \exp\left(\frac{2\sigma \bar{v}_i}{rRT_\infty}\right) \tag{3}$$

The solute effect relates the equilibrium surface pressure of a given component over a flat surface to the liquid fraction of that component by

$$p_{fi} = \gamma_i x_i p_{\text{sat}i} \tag{4}$$

If the component of interest is water, the water activity a_w is often used:

$$p_{fw} = a_w p_{\text{sat}w} \tag{5}$$

Transport and Chemical Reaction Within the Liquid Phase

Since the particles of interest have radii of approximately 1 μm or less, we can assume that the liquid phase is well-mixed, and that diffusion in the particle is rapid compared with other processes taking place. (For a characteristic diffusivity of 10^{-5} cm^2/sec, a characteristic diffusion time of $r^2 \times 10^{-3}$ seconds is obtained, where r is the droplet radius in μm.) Hence, it is necessary only to deal with the pertinent chemistry taking place within the aerosol particle, and we can assume this liquid chemistry occurs homogeneously throughout the particle. This does not discount, however,

TABLE 1. AEROSOL GROWTH CALCULATIONS

Initial aerosol	Pollutants considered	Relative humidity ranges	Liquid phase oxidation mechanism	Reference
Marine aerosol (H_2O, NaCl, $MgCl_2$)	SO_2, O_2, O_3	85-90%	Dissolved O_2, O_3	a
(H_2O, NaCl, $MgCl_2$)	SO_2, NH_3, O_2, O_3	85-99%	Ammonia catalyzed	a
(H_2O, NaCl, $MgCl_2$)	SO_2, NH_3, H_2SO_4	85-99%	Negligible	a
(H_2O, NaCl, $MgCl_2$)	SO_2, NH_3, H_2SO_4, NO, NO_2	88-92%	Negligible	b
Power plant plume (H_2O, $Fe_2(SO_4)_3$)	SO_2, NH_3	95-97%	Metal catalyzed	a

a = Peterson and Seinfeld, 1979.
b = This work.

the possibility of surface-catalyzed chemical reactions, of importance primarily for solid particles.

Chemical reactions within the aerosol particle can be classified as equilibrium or nonequilibrium. Typically, equilibrium reactions include dissociation reactions, and the model employed must utilize equilibrium expressions, electroneutrality constraints, and ionic strength calculations in order to predict concentrations of these dissociation products. The nonequilibrium reactions include (but are not restricted to) oxidation mechanisms for dissolved gases or their equilibrium dissociation products (such as the oxidation of SO_2 to sulfate in a liquid droplet).

Summary of this Work

With this model, a number of studies have been made of the behavior of growing, reacting aerosols. Both initial marine aerosols and power plant plume aerosols have been studied. Table 1 summarizes the initial aerosol for a number of the systems that have been studied using this model. Also shown are the gaseous pollutants considered, relative humidity ranges, and possible liquid phase chemical reactions. In this work we devote our attention to the aqueous sulfate-nitrate system, with particular interest in the simultaneous formation of each species and the resultant effect on particle size and pH.

CHEMICAL MECHANISMS OF SULFATE AND NITRATE FORMATION

The two basic mechanisms for SO_2 oxidation are gas phase photochemical oxidation and liquid phase (possibly catalyzed) oxidation of dissolved SO_2. Sander and Seinfeld (1979) and Calvert et al. (1978) summarize the possible important mechanisms for photochemical SO_2 oxidation. Many authors have dealt with the liquid phase oxidation of SO_2, and Tables 3-5 of Peterson and Seinfeld (1978) summarize many of these. The liquid phase SO_2 oxidation mechanisms fall into two categories: catalyzed and uncatalyzed. In general, the catalyzed SO_2 oxidation rates are much faster than uncatalyzed rates. The most effective catalysts appear to be dissolved trace metals, such as Mn^{2+}, Fe^{3+} and Cu^{2+}, whereas uncatalyzed oxidation mechanisms include SO_2 oxidation by O_2 and O_3 (Larson et al. 1978).

Gaseous oxides of nitrogen (NO and NO_2) can be converted to particulate nitrate through gas phase formation of nitric acid and reaction of the nitric acid and ammonia to form ammonium nitrate or through direct absorption of NO and NO_2 in droplets, followed by conversion of the dissolved NO and NO_2 to NO_3.

Data obtained in the South Coast Air Basin of California suggest that sulfates consistently accumulate in the lower size fraction of ambient aerosols (mass median diameter approximately 0.3 μm) while nitrates seem to exhibit different behavior in the morning than in the afternoon, with nitrate mass median diameters of >0.5 μm and <0.5 μm in the morning and afternoon, respectively. This suggests that the mechanisms governing sulfate and nitrate formation in a photochemical smog environment may be fundamentally different, particularly in the morning. Whereas both homogeneous and heterogeneous mechanisms probably operate for both sulfates and nitrates, we will examine here the combination of gas phase oxidation of SO_2 to H_2SO_4 and liquid phase nitrate formation following absorption of NO and NO_2. Subsequent studies would be needed to evaluate the role of catalysts in SO_2 oxidation. There is evidence that homogeneous nitrate formation takes place by gas phase formation of nitric acid from NO and NO_2, followed by reaction with ammonia to yield solid ammonium nitrate (Stelson et al. 1979). This mechanism, which would tend to yield nitrate-containing particles in the smaller (<0.5 μm diameter) size range, is not examined here.

The equilibrium chemistry of the aqueous system of H_2SO_4, SO_2, NH_3, NO and NO_2 is described in Table 2. Note that the possibility of HCl desorption from the particle (Cl from the dissociated salts) is also included. It can be shown that inclusion of liquid phase SO_2 oxidation in the presence of condensation of H_2SO_4 (formed in the gas phase) has little or no effect on the sulfate content of the particle. Rate of H_2SO_4 condensation on the particle can be written in the form

$$\frac{dm_{H_2SO_4}}{dt} = \frac{1}{1 + lKn} \frac{4\pi r D_{H_2SO_4}}{RT_\infty} p_{\infty_{H_2SO_4}} \qquad (6)$$

where we assume the surface resistance to H_2SO_4 condensation is negligible, due to the extremely low equilibrium vapor pressure of H_2SO_4.

In the next section, we describe the values chosen for the parameters necessary to perform the simulation, present the results of these simulations, and discuss the implications these results have regarding the pollutant levels experienced in the atmosphere.

RESULTS AND DISCUSSION

The simulations were performed to provide information on the variation in concentration of particulate species with the ambient variables, the partial pressures p_{SO_2}, p_{NH_3}, p_{NO} and p_{NO_2}, the sulfuric acid vapor pressure $p_{H_2SO_4}$, the water pressure (or relative humidity) p_{H_2O}, and the initial particle radius r_i. The approach taken here is to first select "reasonable" values for all these

TABLE 2. EQUILIBRIUM CHEMISTRY FOR MARINE AEROSOL GROWTH FROM EXPOSURE TO H_2SO_4, SO_2, NH_3, NO, NO_2, H_2O

	Reaction	Equilibrium constant	Value at 25°C
1.	$H_2O_{(g)} \rightleftarrows H_2O_{(l)}$	$1/P_{satw} = a_w/P_{H2O}$	31.99 atm^{-1}
2.	$H_2O_{(l)} \rightleftarrows H^+ + OH^-$	$K_w = [H^+]\,[OH^-]\,\gamma_+\gamma_-$	10^{-14} $moles^2\,l^{-2}$
3.	$SO_{2(g)} \rightleftarrows SO_{2(l)}$	$K_{hs} = [SO_{2(l)}]/P_{SO2}$	1.24 moles l^{-1} atm^{-1}
4.	$SO_{2(l)} \rightleftarrows H^+ + HSO_3^-$	$K_{1s} = [H^+]\,[HSO_3^-]\,\gamma_+\gamma_-/[SO_{2(l)}]$	0.0127 moles l^{-1}
5.	$HSO_3^- \rightleftarrows H^+ + SO_3^=$	$K_{2s} = [H^+]\,[SO_3^=]\,\gamma_+\gamma_2-/[HSO_3^-]\gamma_-$	6.24×10^{-8} moles l^{-1}
6.	$NH_{3(g)} \rightleftarrows NH_{3(l)}$	$K_{ha} = [NH_{3(l)}]/P_{NH3}$	57 moles l^{-1} atm^{-1}
7.	$NH_{3(l)} \rightleftarrows NH_4^+ + OH^-$	$K_{1a} = [NH_4^+]\,[OH^-]\,\gamma_+\gamma_-/[NH_{3(l)}]$	1.774×10^{-5} moles l^{-1}
8.	$NO_{(g)} + NO_{2(g)} + H_2O \rightleftarrows 2HNO_2$	$K_{1n} = [HNO_2]^2/P_{NO}P_{NO2}$	122 $moles^2\,l^{-2}\,atm^{-2}$
9.	$2NO_{2(g)} + H_2O \rightleftarrows HNO_2 + H^+ + NO_3^-$	$K_{2n} = [HNO_2]\,[H^+]\,[NO_3^-]\,\gamma_+\gamma_-/P^2_{NO2}$	4.3×10^5 $moles^3\,l^{-3}\,atm^{-2}$
10.	$HNO_2 \rightleftarrows H^+ + NO_2^-$	$K_{3n} = [H^+]\,[NO_2^-]\,\gamma_+\gamma_-/[HNO_2]$	5.1×10^{-4} moles l^{-1}
11.	$MgCl_2 \rightleftarrows Mg^{++} + 2Cl^-$	$K_{1m} = [Mg^{++}]\,[Cl^-]^2\,\gamma_{2+}\gamma_{-2}/[MgCl_{2(l)}]$	∞
12.	$NaCl \rightleftarrows Na^+ + Cl^-$	$K_{1Na} = [Na^+]\,[Cl^-]\,\gamma_+\gamma_-/[NaCl_{(l)}]$	∞
13.	$HCl_{(g)} \rightleftarrows HCl_{(l)}$	$K_{hh} = [HCl_{(l)}]/P_{HCl}$	19 moles l^{-1} atm^{-1}
14.	$HCl_{(l)} \rightleftarrows H^+ + Cl^-$	$K_{1H} = [H^+]\,[Cl^-]\,\gamma_+\gamma_-/[HCl_{(l)}]$	1.3×10^6 moles l^{-1}

parameters (as they pertain to conditions found, for example, in the Los Angeles atmosphere) and use these values to compute a base case. We chose to maintain the vapor concentrations constant in time, to emphasize only the effects on particle growth and chemical reaction of changing various parameters of the system, such as relative humidity and initial particle size. Each parameter is then systematically varied (within expected atmospheric limits), and the effect of these variations on particle growth and chemical change is studied.

Table 3 lists the parameter values chosen for the base case and for all subsequent cases studied. Levels of p_{SO2}, p_{NH3}, p_{NO} and p_{NO2} were based on values experienced in the Los Angeles area. The value for p_{H2SO4} was estimated by Jerskey et al. (1978) by equating the rate of conversion of SO_2 to H_2SO_4 to the rate of condensation (based on typical aerosol surface area measurements) to the aerosol phase.

The high values selected for relative humidity ($p_{satw} \simeq$ 31 000 ppm) were necessary in order to calculate water activity of the particle. Calculation of water activity of a multicomponent droplet relies (in this work) on the water activities of reported binary solutions. Since, at equilibrium, the relative humidity equals the water activity (or is slightly higher if the Kelvin effect is important), binary water activity data must be available for water activities down to the *lowest* relative humidity to be considered. Typically, most water activity data for compounds of interest in particulate air pollution problems pertain only to dilute solutions (and hence water activities near 1.0). We therefore consider only cases of high relative humidities. It is important to realize, however, that this is *not* a limitation of the model, but rather a limitation brought about by lack of sufficient thermodynamic data.

Run A in Table 3 is the base case against which all other cases will be compared. Relative humidity is increased (from 90% to 91%)* in Run B, while the ammonia pressure is lowered in Run C. The H_2SO_4 pressure is lowered in Run D. The NO pressure is increased in Run E, while the NO_2 pressure is decreased in Run F. Finally, both NO and NO_2 pressures are set to zero in Run G.

Before studying the specific effects of varying these parameters on the size and composition of individual particles, it is worthwhile to look at the effect of *initial* particle radius on evolution of particle size and composition. In addition, it is useful to study the evolution of a postulated initial particle size distribution. To accomplish this, conditions identical to the base case in Table 3 (Run A), but with varying initial particle radius, are simulated. Selected initial particle sizes are obtained by varying initial salt composition of the marine aerosol assumed in equilibrium with the ambient relative humidity.

Figure 1 shows the fractional composition of $[SO_4^=]$, $[NO_3^-]$ and $[NH_4^+]$ within the particle as a function of particle radius at $t = 2$ hours. While these concentrations will change for longer times, the trends remain the same. Here, $[NO_3^-]$ increases as particle radius increases; both $[SO_4^=]$ and $[NH_4^+]$ decrease as particle radius increases. For the mechanisms chosen, sulfates seem to favor the smaller particles, while nitrates favor the larger particles.

Figure 2 demonstrates how a hypothetical aerosol distribution would evolve under the influence of the mechanisms outlined here. Chosen as an initial distribution is

$$n(r) = \frac{4N_o}{r_o}\left(\frac{r}{r_o}\right)\exp(-2r/r_o) \qquad (7)$$

where $n(r)dr$ is the number of particles per cm^3 in the size range $(r, r + dr)$. The number of particles greater than size r, $N(r)$, is thus

$$\frac{N(r)}{N_o} = \left(1 + \frac{2r}{r_o}\right)\exp(-2r/r_o) \qquad (8)$$

Figure 2 shows $N(r)/N_o$ vs r (assuming $r_o = 0.3$ μm) at time $t = 0$, and the evolution of this particle size distribution with time as the aerosol undergoes simultaneous growth and chemical reaction. There is the characteristic shift to larger sizes, accompanied by a sharp, almost monodisperse behavior in the distribution. This is typical of condensational growth into the "accumulation mode" of the distribution. The accumulation mode of a distribution is characterized by particles resulting from secondary aerosol formation on existing nuclei.

It should be noted that the relative (rather than absolute) characteristics of the size distribution can be studied in Figure 2. In selecting a value for r_o in Equation 7, the peak of the distribution can be shifted to larger or smaller sizes. The model utilized describes the growth of a particle from one particle size to another. From an initial distribution, and by assuming all particle size distribution change is due to condensational growth, we

* The small changes in relative humidity are necessary because 1) thermodynamic data limitations prevent lower relative humidities from being considered, and 2) rapid increases in growth rate with relative humidity make high relative humidity conditions (≥ 95% RH) physically unrealistic.

TABLE 3. PARAMETERS FOR MARINE AEROSOL GROWTH FROM EXPOSURE TO H_2SO_4, SO_2, NH_3, NO, NO_2, H_2O

Run	r_i (μm)	p_{H_2O} (ppm)	p_{SO_2} (ppm)	p_{NH_3} (ppm)	$p_{H_2SO_4}$ (ppm)	p_{NO} (ppm)	p_{NO_2} (ppm)	Remarks
A	0.1	28,140	0.01	0.01	5.E-6	0.1	0.05	Base case
B	0.1	28,450	0.01	0.01	5.E-6	0.1	0.05	RH increased
C	0.1	28,140	0.01	0.001	5.E-6	0.1	0.05	P_{NH_3} decreased
D	0.1	28,140	0.01	0.01	5.E-7	0.1	0.05	$P_{H_2SO_4}$ decreased
E	0.1	28,140	0.01	0.01	5.E-6	0.2	0.05	P_{NO} increased
F	0.1	28,140	0.01	0.01	5.E-6	0.1	0.01	P_{NO_2} decreased
G	0.1	28,140	0.01	0.01	5.E-6	1.E-50	1.E-50	P_{NO}, P_{NO_2}, ~ 0

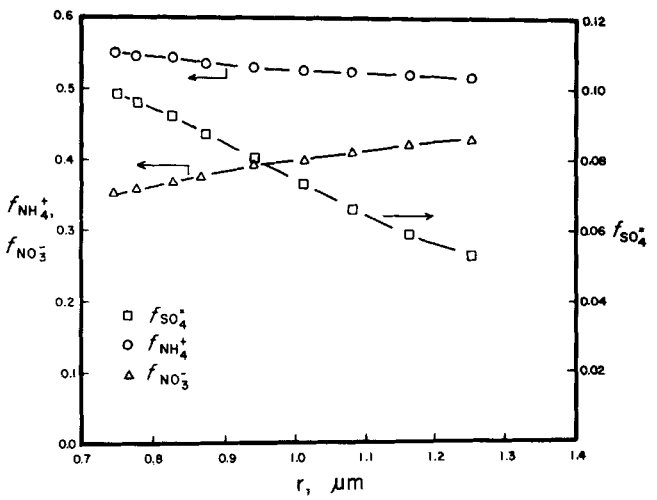

Figure 1. $f_{SO_4^=}$, $f_{NH_4^+}$ and $f_{NO_3^-}$ versus particle size at $t = 2$ hours, for "base case" runs (A, Table 3) of varying initial particle radius.

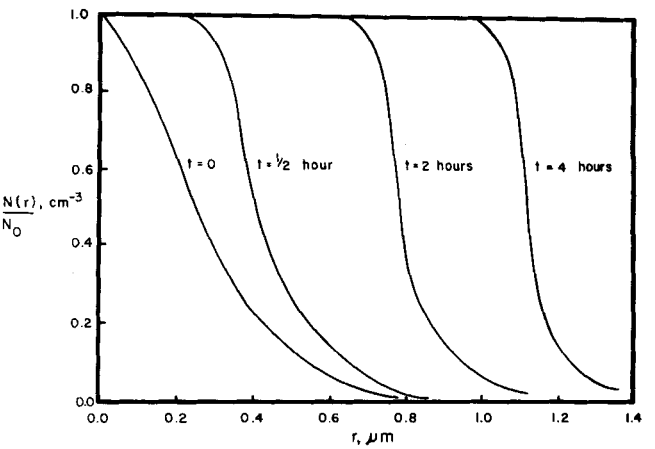

Figure 2. Fracture of particles greater than r for $t = 0$, 1/2, 2 and 4 hours, respectively, for "base case" runs (A, Table 3) of varying initial particle radius.

can determine the size distribution of the aerosol for all times.

Figures 3 through 7 describe the variation of particle radius, pH, sulfate concentration, nitrate concentration and ammonium concentration as a function of exposure time to the various gaseous pollutants and water vapor.

From Figure 3, in the base case (A), an increase in particle radius occurs from an initial 0.1 μm to approximately 1.5 μm in 120 min. Increasing relative humidity (B) causes a large increase in the *rate* of particle growth. This is expected since, to maintain thermodynamic equilibrium at higher humidities, proportionally larger amounts of water must be added to the droplet as sulfuric acid

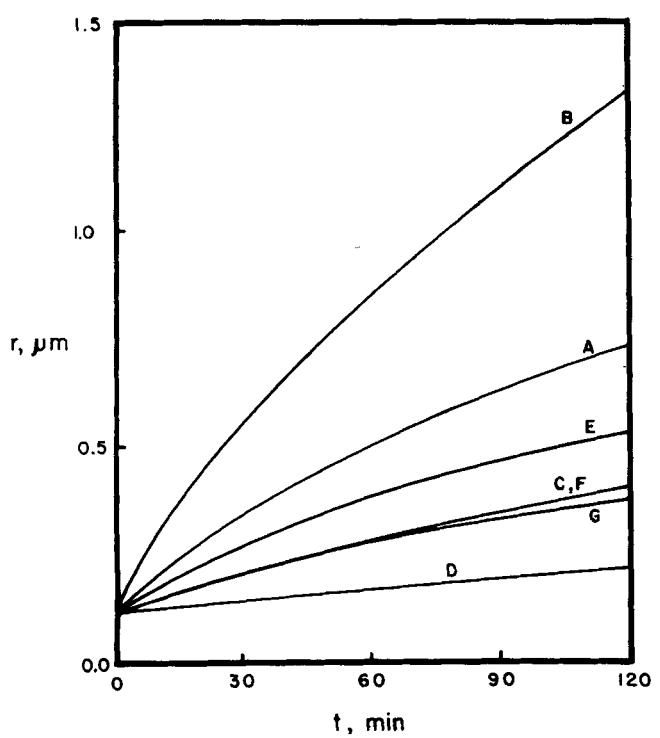

Figure 3. Temporal variation of particle radius for (A) base case, (B) increased relative humidity, (C) decreased p_{NH_3}, (D) decreased $p_{H_2SO_4}$, (E) increased p_{NO}, (F) decreased p_{NO_2} and (G) $p_{NO} = p_{NO_2} = 0$. Parameter values listed in Table 3.

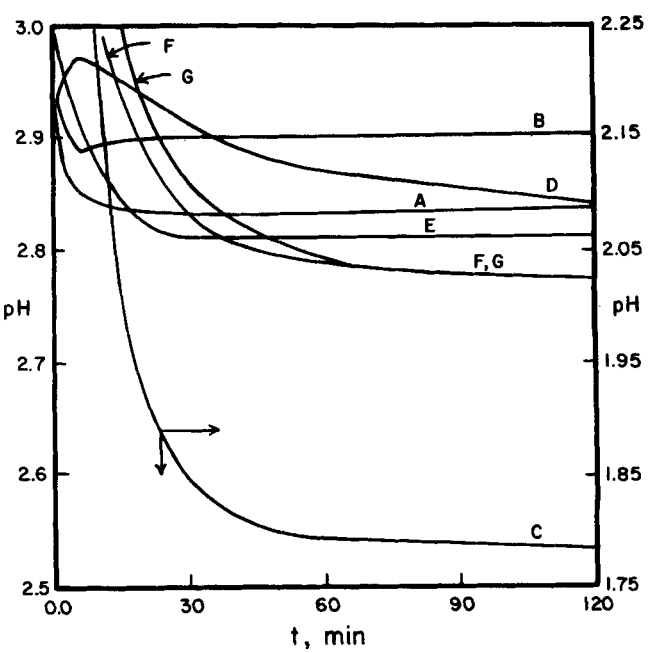

Figure 4. Temporal variation of particle pH for (A) base case, (B) increased relative humidity, (C) decreased p_{NH_3}, (D) decreased $p_{H_2SO_4}$, (E) increased p_{NO}, (F) decreased p_{NO_2} and (G) $p_{NO} = p_{NO_2} = 0$. Parameter values listed in Table 3.

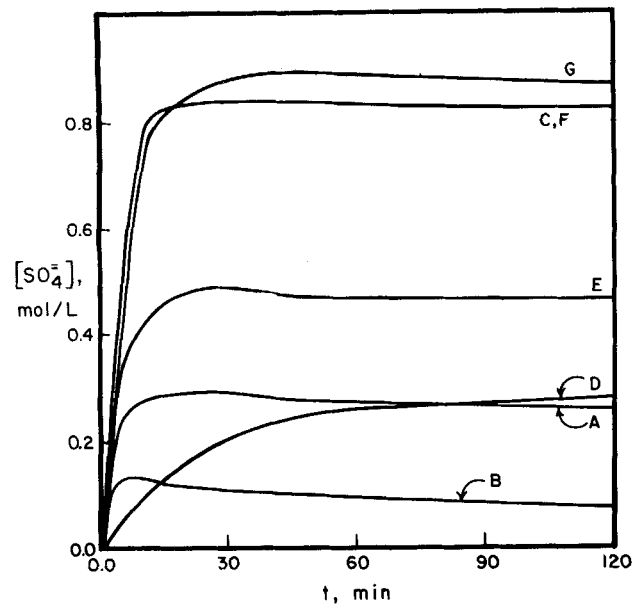

Figure 5. Temporal variation of particle $[SO_4^{=}]$ for (A) base case, (B) increased relative humidity, (C) decreased p_{NH_3}, (D) decreased $p_{H_2SO_4}$, (E) increased p_{NO}, (F) decreased p_{NO_2} and (G) $p_{NO} = p_{NO_2} = 0$. Parameter values listed in Table 3.

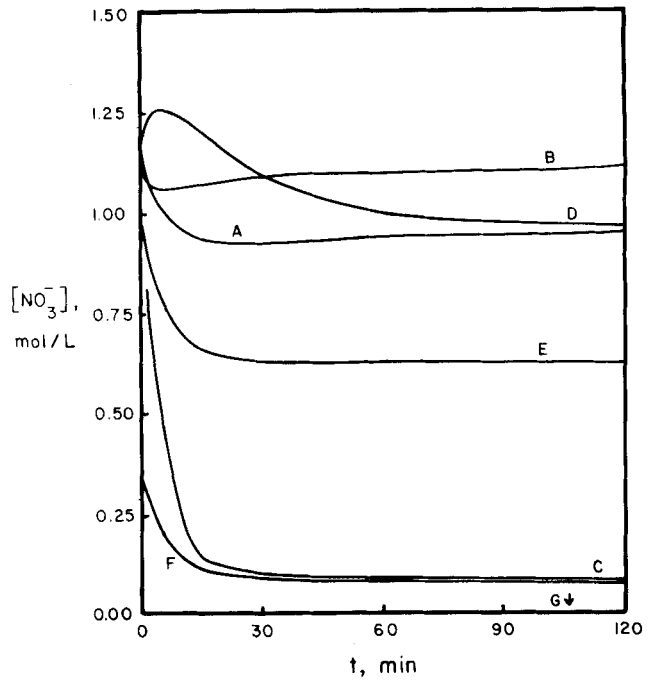

Figure 6. Temporal variation of particle $[NO_3^{-}]$ for (A) base case, (B) increased relative humidity, (C) decreased p_{NH_3}, (D) decreased $p_{H_2SO_4}$, (E) increased p_{NO}, (F) decreased p_{NO_2} and (G) $p_{NO} = p_{NO_2} = 0$. Parameter values listed in Table 3.

condenses. Decreasing p_{NH_3} (C) causes a slowing of the growth rate for two reasons. First, the initial ammonium level drops, raising the water activity. Second, the pH decreases as p_{NH_3} decreases, causing a decrease in $[NO_3^{-}]$. This also raises the water activity, and hence, lowers the driving force for growth. Lowering $p_{H_2SO_4}$ (D) causes a decrease in the growth rate, again due to the effect on water activity. Similarly, raising p_{NO} (E) and lowering p_{NO_2} (F) cause slowed growth rates, because of the nitrate dependence on p_{NO} and p_{NO_2} ($[NO_3^{-}] \propto p_{NO_2}^{3/2} p_{NO}^{-1/2}$). Setting $p_{NO} = p_{NO_2} = 0$ (G) affects growth rate similarly.

Figure 4 describes the variation of particle pH with exposure time. In the base case (A), a particle pH of about 2.8 is achieved for exposure times greater than 30 min. Increasing relative humidity (B) raises pH for a given time, due to dilution of an acidic particle. Lowering p_{NH_3} (C) has the expected dramatic effect on lowering pH, which approaches 1.75 for long times. Decreasing $p_{H_2SO_4}$ (D) lowers the *rate* of H_2SO_4 condensation, and hence the rate of decrease in pH, but for long time the pH approaches the level found in Case A. Although less sulfuric acid is condensed, the rate of water added to maintain thermodynamic equilibrium is also decreased, so that particle pH, for long times, remains essentially the same. Increasing p_{NO} (E), decreasing p_{NO_2} (F) and setting both to zero (G) cause the $[NO_3^{-}]$ level to drop (as will be seen in Figure 6). In so doing, water activity increases and particle growth rate slows as in Figure 3. Hence, a higher concentration of an acidic solution causes the pH to drop.

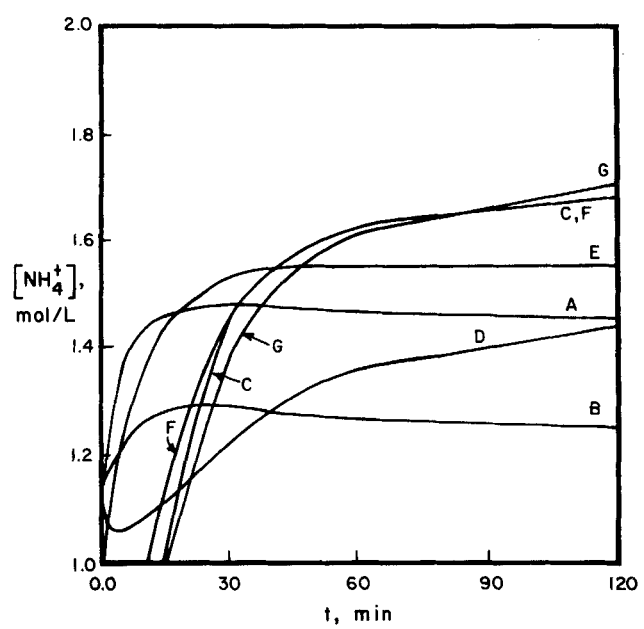

Figure 7. Temporal variation of particle $[NH_4^{+}]$ for (A) base case, (B) increased relative humidity, (C) decreased p_{NH_3}, (D) decreased $p_{H_2SO_4}$, (E) increased p_{NO}, (F) decreased p_{NO_2} and (G) $p_{NO} = p_{NO_2} = 0$. Parameter values listed in Table 3.

Figure 5 describes the $[SO_4^{=}]$ level as a function of exposure time. Increasing relative humidity (B) decreases the $[SO_4^{=}]$ level, due to dilution. A decrease in p_{NH_3} (C), by lowering the pH, decreases $[NO_3^{-}]$ and increases water activity. This causes the particle

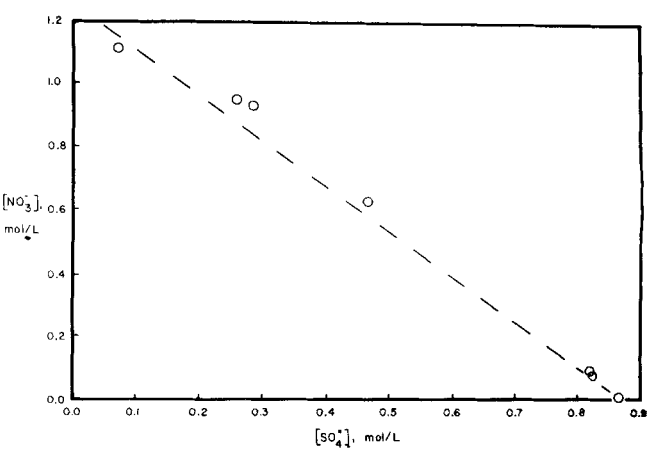

Figure 8. Predicted levels of $[NO_3^{-}]$ vs. $[SO_4^{=}]$ at $t = 3$ hours for all simulations listed in Table 3.

to grow more slowly and to yield higher $[SO_4^=]$ levels. Decreasing $p_{H_2SO_4}$ (D) slows the *rate* of increase of $[SO_4^=]$, but does not drastically affect the $[SO_4^=]$ value for long times. Increasing p_{NO} (E), decreasing p_{NO_2} (F) and setting both to zero (G) "concentrates" the particle, due to the water activity dependence previously discussed.

Figure 6 describes the variation of $[NO_3^-]$ with exposure time. Increasing relative humidity (B) leads to sulfate dilution, raising the pH (as seen in Figure 4) and hence increasing $[NO_3^-]$. Decreasing p_{NH_3} (C) causes pH, and then $[NO_3^-]$, to drop. Decreasing $p_{H_2SO_4}$ (D) causes an initial drop in $[SO_4^=]$ and an increase in $[NO_3^-]$, but as $[SO_4^=]$ nears the level found in the base case (A) (Figure 5), $[NO_3^-]$ does likewise. Increasing p_{NO} (E), decreasing p_{NO_2} (F) and setting both to zero (G) have the obvious effect on $[NO_3^-]$—a significant lowering of the equilibrium levels.

Figure 7 describes the variation of $[NH_4^+]$ with exposure time. Increasing relative humidity (B) lowers pH by dilution, and hence $[NH_4^+]$ is lowered. Quite opposite from what intuition would lead one to expect, decreasing p_{NH_3} (C) actually *increases* $[NH_4^+]$. The $[NH_4^+]$ level varies linearly both with p_{NH_3} and with $[H^+]$. Initially, $[NH_4^+]$ is much lower than the base case (A). However, due to H_2SO_4 condensation, pH decreases until the decrease in pH (increase in $[H^+]$) outweighs the decrease in p_{NH_3}, and $[NH_4^+]$ goes up. Decreasing $p_{H_2SO_4}$ (D) causes the *rate* of increase in $[SO_4^=]$ to slow; hence the *rate* of decrease in pH also slows (Figure 4). It does not significantly affect the pH for long times, and hence not the $[NH_4^+]$ level, for long times. Increasing p_{NO} (E), decreasing p_{NO_2} (F) and setting both to zero (G), as we have already seen (Figure 3), slow the particle growth rate and hence decrease pH. This causes the $[NH_4^+]$ level to rise, due to linear dependence of $[NH_4^+]$ on $[H^+]$.

From Figures 3 through 7, ion concentrations reach almost constant levels within a period of two to three hours or less. For this reason, it is useful to compare these "long-time" values for different ions—to sulfate and nitrate ions in particular. In so doing, any possible relationship between ions (for the mechanism proposed and the parameters considered) can be seen.

Figure 8 shows nitrate concentration vs. sulfate concentration at $t = 3$ hours for all simulations. While there is some scatter in the results, a definite inverse correlation between sulfate and nitrate concentration exists. In other words, those parameters which cause the nitrate concentration to increase will cause the sulfate concentration to decrease, and visa versa. In Figure 6, increasing relative humidity, p_{NO_2} or p_{NH_3} will cause the nitrate concentration to increase. Higher relative humidities and higher p_{NH_3} levels both increase particle pH, which facilitates equilibrium nitrate formation. Higher p_{NO_2} levels also shift the equilibrium nitrate level to higher concentrations.

High sulfate concentrations, on the other hand, are a consequence of higher $p_{H_2SO_4}$ and p_{NO} levels. Since the mechanism of sulfate formation considered here is gas phase oxidation to sulfuric acid and subsequent condensation, increasing $p_{H_2SO_4}$ raises the driving force for H_2SO_4 condensation. The increase in $[SO_4^=]$ with p_{NO} is not as obvious. As p_{NO} goes up, equilibrium $[NO_3^-]$ decreases, thus increasing water activity and slowing the growth rate. Since H_2SO_4 condensation is insensitive to particle properties (due to the low equilibrium vapor pressure of H_2SO_4), a slower growth rate yields higher $[SO_4^=]$ levels.

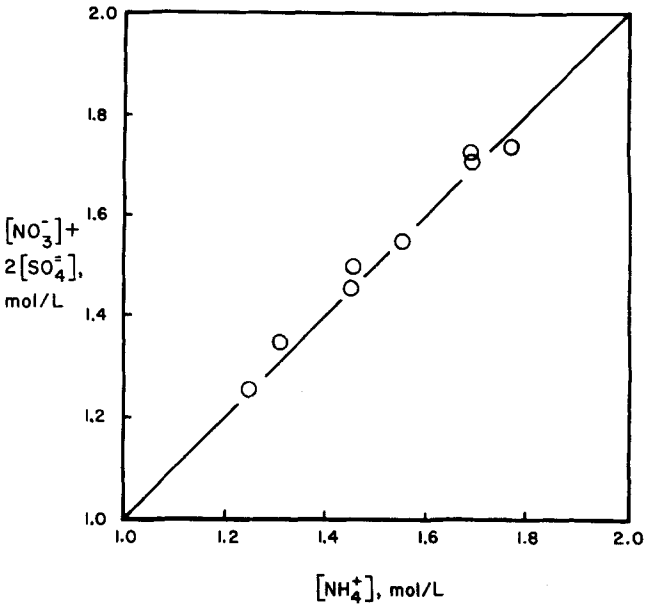

Figure 9. Predicted levels of the sum $[NO_3^-] + 2[SO_4^=]$ vs. $[NH_4^+]$ at $t = 3$ hours for all simulations listed in Table 3.

There is much speculation as to the speciation of $[SO_4^=]$, $[NO_3^-]$ and $[NH_4^+]$ in the aerosol particle. Figure 9 presents evidence for the possibility of both sulfate and nitrate existing as their ammonium salts. Plotted in Figure 9 is the sum: $2[SO_4^=] + [NO_3^-]$ vs. $[NH_4^+]$, which, if all sulfate and nitrate were present as $(NH_4)_2SO_4$ and NH_4NO_3, would yield a straight line of slope 1. The simulations indicate that $[NH_4^+]$, $[NO_3^-]$ and $[SO_4^=]$ are near-stoichiometric.

The following conclusion can be drawn from this figure: If the mechanisms of sulfate and nitrate formation are condensation of H_2SO_4 vapor and equilibrium NO—NO_2 dissolution, respectively, the ratio of $[SO_4^=]$ and $[NO_3^-]$ to $[NH_4^+]$ is near-stoichiometric. Further, the presence of near-stoichiometric conditions is relatively insensitive to gas phase concentrations of H_2SO_4, NO, NO_2 and NH_3, relative humidities, initial particle radius and the like, for the range of parameters considered here.

While our calculations represent the growth process for a single aerosol particle, it is possible to make qualitative comparisons between the predicted chemical composition and that found in the atmosphere. The most meaningful comparison is between relative sulfate, nitrate and ammonium levels. As shown in Figure 9, a near-stoichiometric ratio exists between $[NH_4^+]$ and the sum: $[NO_3^-] + 2[SO_4^=]$. Although not shown here, Peterson and Seinfeld (1979) demonstrated in separate calculations that this stoichiometric relationship does not necessarily hold if liquid phase SO_2 oxidation dominates gas phase SO_2 oxidation. Under those circumstances, the ratio $[NH_4^+]/(2[SO_4^=] + [NO_3^-])$ is on the order of 0.65 or less.

These predictions compare to an average ratio of approximately 0.52 reported by Kadowaki (1976) for the Nagoya, Japan area, and an average ratio of approximately 0.87 reported by Appel et al. (1978) for the Los Angeles area. These data indicate that a liquid phase SO_2 oxidation mechanism may be of importance in the Nagoya area, whereas a combination of both liquid phase and gas phase SO_2 oxidation mechanisms may be important in the Los Angeles area. Further study into different mechanisms of sulfate and nitrate formation is necessary, however, before any conclusive statements can be made regarding the dominant processes of secondary particle formation.

CONCLUSIONS

The model developed allows the study of aerosol growth and chemical reaction of particles exposed to various gaseous pollutants and condensing vapors. While, for this study, we have assumed the ambient gas phase concentrations to be constant, it is also possible to consider the case in which gaseous concentrations change with time as a result of dispersion as well as gas-to-particle conversion.

For the system considered, namely the exposure of an initial marine aerosol to SO_2, NH_3, NO, NO_2 and H_2SO_4 vapor, we conclude:

1. If a gas phase sulfate formation mechanism and a liquid phase nitrate formation mechanism is employed. equilibrium conditions dictate that the ratio of nitrate and sulfate to ammonium ion is nearly that found in NH_4NO_3 and $(NH_4)_2SO_4$. If however, the sulfate formation mechanism is dominated by liquid phase SO_2 oxidation, it can be shown that this stoichiometric relationship no longer holds.

2. Relative humidity affects the "dilution" of the particulate pollutants within the particle, as well as the size of the particle. Dilution will not directly affect the concentration of ions involved in equilibrium chemical reactions, but could indirectly affect these concentrations through the influence on non-equilibrium ionic concentrations (such as $[SO_4^=]$) on particle pH.

3. Due to this dilution effect, smaller particles tend to be more acidic than larger particles.

4. For the mechanisms chosen to describe the nitrate and sulfate formation rates, those parameters which tend to increase nitrate levels also tend to decrease sulfate levels, and vice versa. Specifically, $[NO_3^-]$ increases with increasing initial particle radius, relative humidity, p_{NO_2} and p_{NH_3}, and decreases with increasing $p_{H_2SO_4}$ and p_{NO}. On the other hand, $[SO_4^=]$ increases with increasing p_{NO} and $p_{H_2SO_4}$, and decreases with increasing p_{NH_3}, p_{NO_2}, relative humidity and initial particle radius.

ACKNOWLEDGMENT

This work was supported by National Science Foundation grants ENV76-04179 and ENG78-05414.

NOTATION

a_w = water activity
D, D_i = binary diffusivity in air, cm²/sec
$f_{SO_4^=} = [SO_4^=]/([SO_4^=] + [NO_3^-] + [NH_4^+])$, dimensionless
$f_{NO_3^-} = [NO_3^-]/([SO_4^=] + [NO_3^-] + [NH_4^+])$, dimensionless
$f_{NH_4^+} = [NH_4^+]/([SO_4^=] + [NO_3^-] + [NH_4^+])$, dimensionless
Kn = Knudsen number, $Kn = \lambda/r$
l = noncontinuum correction factor, Eq. 2
m, m_i = moles of species in aerosol particle, gmoles
$n(r)$ = particle number density, $cm^{-3}\ cm^{-1}$
$N(r)$ = particle concentration for radii greater than or equal to r, cm^{-3}
N_o = total number concentration, cm^{-3}
p_c, p_{ci} = pressure above a curved surface, atm
p_f, p_{fi} = pressure above a flat surface, atm
p_{sat}, p_{sat_i} = saturation vapor pressure, atm
$p_\infty, p_{\infty i}$ = ambient pressure, atm
r = particle radius, cm
r_i = initial particle radius, cm
r_o = mean particle radius, cm
R = gas constant, ergs/gmole °K
T_∞ = ambient temperature, °K
$\bar{v}_i$ = molar volume, cm³/gmole
x_i = mole fraction
γ_i = activity coefficient
λ = mean free path, cm
σ = particle surface tension, ergs/cm²
$[\cdot]$ = concentration, gmoles/cm³

LITERATURE CITED

Appel, B. R., E. L. Kothny, E. M. Hoffer, G. M. Hidy and J. J. Wesolowski, "Sulfate and Nitrate Data from the California Aerosol Characterization Experiment (ACHEX)," *Environ. Sci. Technol.*, **12**, 418 (1978).

Brock, J. R., "Diffusion to Particles in the Near Free Molecule Region," *J. Coll. Int. Sci.*, **22**, 513 (1966).

Calvert, J. G., F. Su, J. W. Bottenheim, and O. P. Strausz, "The Mechanism of the Homogeneous Oxidation of Sulfur Dioxide in the Troposphere," *Atmos. Environ.*, **12**, 1 (1978).

Charlson, R. J., A. H. Vanderpol, D. S. Covert, A. P. Waggoner, and N. C. Ahlquist, "$H_2SO_4/(NH_4)_2SO_4$ Background Aerosol: Optical Detection in St. Louis Region," *Atmos. Environ.*, **8**, 1257 (1974).

Fuchs, N. A., *Evaporation and Droplet Growth in Gaseous Media*, Pergamon Press, Oxford (1959).

Gordon, R. J. and R. J. Bryan, "Ammonium Nitrate in Airborne Particles in Los Angeles," *Env. Sci. Technol.*, **7** (7), 645 (1973).

Jerskey, T. N., J. H. Seinfeld, F. Gelbard and L. E. Reid, "Continued Research in Mesoscale Air Pollution Simulation Modeling: Vol. VII—Mathematical Modeling of Urban Aerosol Dynamics," U.S. Environmental Protection Agency, in press.

Kadowaki, S., "Size Distribution of Atmospheric Total Aerosols, Sulfate, Ammonium and Nitrate Particulates in the Nagoya Area," *Atmos. Environ.*, **10**, 39 (1976).

Larson, T. W., N. R. Horike and H. Harrison, "Oxidation of SO_2 by O_2 and O_3 in Aqueous Solution," *Atmos. Environ.*, **12**, 1597 (1978).

Moskowitz, A. H., "Particle Size Distribution of Nitrate Aerosols in the Los Angeles Air Basin," U.S. Environmental Protection Agency report EPA-600/3-77-053 (May, 1977).

Orel, A. E., and J. H. Seinfeld, "Nitrate Formation in Atmospheric Aerosols," *Environ. Sci. Technol.*, **11** (10), 1000 (1977).

Peterson, T. W., and J. H. Seinfeld, "Heterogeneous Condensation and Chemical Reaction in Droplets—Application to the Heterogeneous Atmospheric Oxidation of SO_2," *Adv. Environ. Sci. Technol.*, in press.

Sahni, D. C., "The Effect of a Black Sphere on the Flux Distribution in an Infinite Moderator," *J. Nucl. Eng. A/B*, **20**, 915 (1966).

Sampson, R. E. and G. S. Springer, "Condensation on and Evaporation from Droplets by a Moment Method," *J. Fluid Mech.*, **36** (3), 577 (1969).

Sandberg, J. S., D. A. Levaggi, R. E. DeMandel, and W. Siu, "Sulfate and Nitrate Particulates as Related to SO_2 and NO_x Gases and Emissions," *J. Air Pollut. Control Assoc.*, **26** (6), 559 (1976).

Sander, S. P. and J. H. Seinfeld, "Chemical Kinetics of Homogeneous Atmospheric Oxidation of SO_2," *Environ. Sci. Technol.*, **10** (12), 1114 (1976).

Shankar, P. N., "A Kinetic Theory of Steady Condensation," *J. Fluid Mech.*, **40** (2), 385 (1970).

Stelson, A. W., S. K. Friedlander, and J. H. Seinfeld, "A Note on the Equilibrium Relationship Between Ammonia and Nitric Acid and Particulate Ammonium Nitrate," *Atmos. Environ.*, 13, 369 (1979).

Manuscript received September 11, 1978; revision received May 23, and accepted June 5, 1979.